Multi-Scale Synthesis of Reflectarrays Exploiting the SbD Paradigm

G. Oliveri, A. Gelmini, A. Polo, N. Anselmi, and A. Massa

Contents

1 Problem Formulation

1.1 Geometrical Description

We define two reference systems as in Fig. 1:

- Global Reference System (GRS): defined in $(x',\, y',\, z')$ with:
  - Feed position in $(x'_F,\, y'_F,\, z'_F)$
  - Cell position in $(x'_C,\, y'_C,\, z'_C)$
- Local Reference System (LRS): defined in $(x,\, y,\, z)$ with:
  - Feed position in $(x_F,\, y_F,\, z_F)$
  - Cell position in $(0,\, 0,\, 0)$
- Angle of Incidence of Feed Wave:
  - $\theta_{inc} = \arccos\left(\frac{z_F}{\sqrt{x_F^2+y_F^2+z_F^2}}\right)$
  - $\phi_{inc} = \arctan\left(\frac{y_F}{x_F}\right)$

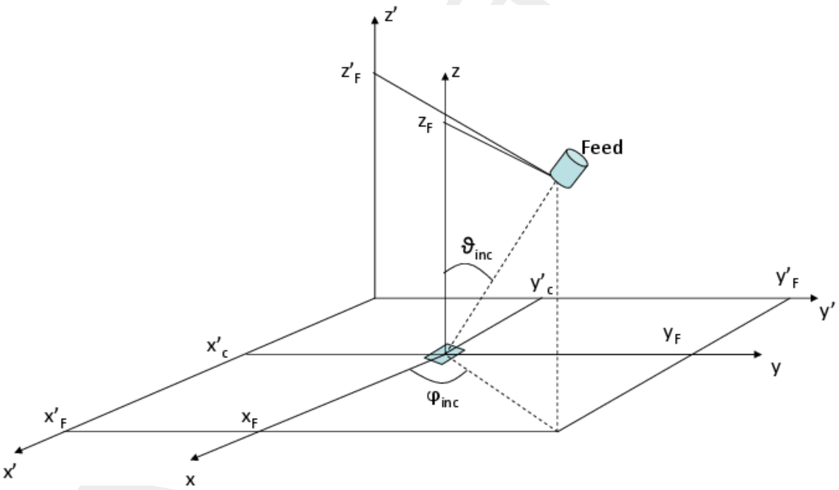

Figure 1: Geometrical description of the problem - Local and Global reference Systems.

1.2 Incident Field in LRS

The incident field in the LRS can be expressed as:

$$\mathbf{E}_{inc} = \left(E^{\theta}_{inc}\underline{\hat{\theta}} + E^{\phi}_{inc}\underline{\hat{\phi}}\right)\exp\left(-jk_0\underline{\hat{\mu}}_{inc}\cdot\underline{r}\right) \quad (1)$$

where:

- $k_0 = 2\pi/\lambda$: is the wave number;
- $\underline{\hat{\mu}}_{inc} = -\left(\sin\left(\theta_{inc}\right)\cos\left(\phi_{inc}\right),\, \sin\left(\theta_{inc}\right)\sin\left(\phi_{inc}\right),\, \cos\left(\theta_{inc}\right)\right)$: is the propagation vector;

1.3 Floquet analysis

Since we assum a Floquet analysis truncate at the first term (only 1 TE/TM mode) we can define:

$$\begin{bmatrix} E^{\theta}_{inc} \\ E^{\phi}_{inc} \end{bmatrix} = \begin{bmatrix} E^{TM}_{inc} \\ E^{TE}_{inc} \end{bmatrix} \tag{2}$$

1.4 Scattered Field

Given the scattering matrix (S) in output from HFSS (Floquet first order approaximation) the scattered field can be computed as:

$$\begin{bmatrix} E^{TM}_{scat} \\ E^{TE}_{scat} \end{bmatrix} = [S] \begin{bmatrix} E^{TM}_{inc} \\ E^{TE}_{inc} \end{bmatrix} \tag{3}$$

1.5 The Surface current computation

The surface current on the reflectarray aperture can be computed from the incident and scattered field as:

$$\begin{aligned} \mathbf{J}_s\left(\underline{r}\right) &= \underline{\hat{n}} \times \mathbf{H}_{TOT}\left(\underline{r}\right) \\ \mathbf{M}_s\left(\underline{r}\right) &= -\underline{\hat{n}} \times \mathbf{E}_{TOT}\left(\underline{r}\right) \end{aligned} \tag{4}$$

where:

- $\mathbf{H}_{TOT} = \mathbf{H}_{inc} + \mathbf{H}_{scat}$
- $\mathbf{E}_{TOT} = \mathbf{E}_{inc} + \mathbf{E}_{scat}$

But we need to have the fields expressed in cartesian components.

1.6 From spherical to cartesian components

This procedure is standard and is valid both for incident and scattered field:

$$\begin{bmatrix} E^{x}_{inc/scat} \\ E^{y}_{inc/scat} \\ E^{z}_{inc/scat} \end{bmatrix} = \begin{bmatrix} \sin\left(\theta_{inc}\right)\cos\left(\phi_{inc}\right) & \cos\left(\theta_{inc}\right)\cos\left(\phi_{inc}\right) & -\sin\left(\phi_{inc}\right) \\ \sin\left(\theta_{inc}\right)\sin\left(\phi_{inc}\right) & \cos\left(\theta_{inc}\right)\sin\left(\phi_{inc}\right) & \cos\left(\phi_{inc}\right) \\ \cos\left(\theta_{inc}\right) & -\sin\left(\theta_{inc}\right) & 0 \end{bmatrix} \begin{bmatrix} 0 \\ E^{TM}_{inc/scat} \\ E^{TE}_{inc/scat} \end{bmatrix} \tag{5}$$

1.7 Summary of the procedure

1. From a FEKO simulation of a feeder we obtain the Electric incident field in cartesian components;
2. We derive the spherical (and also TE/TM) components of the Electric incident field;
3. We compute the Electric scattered field;

4. From the incident and scattered Electric field we derive the Magnetic field as:

$$\mathbf{H}_{inc/scatt} = \frac{1}{\eta}\underline{\hat{\mu}}_{inc/scat} \times \mathbf{E}_{inc/scatt} \tag{6}$$

5. Compute the Electric Currents from the total Magnetic Field.

2 Preliminary Results: Square Patch Reflectarray: 25x25

2.1 Unit cell geometry

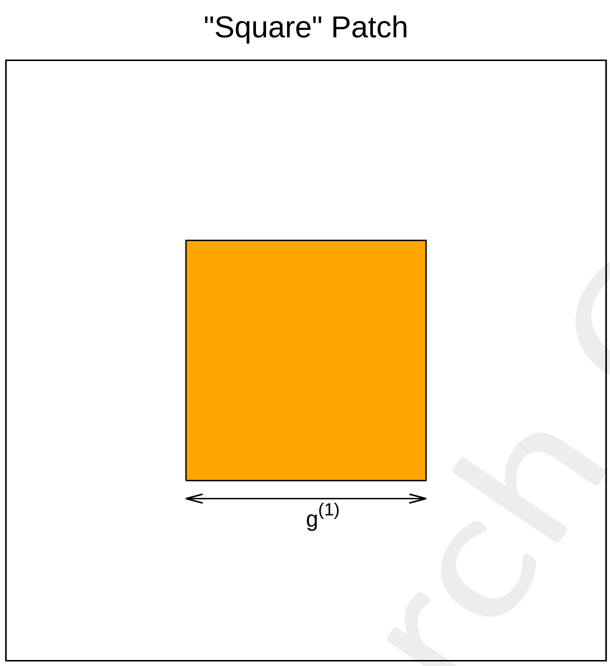

Figure 2: Square Patch unit cell.

2.2 Accuracy vs. Training Samples

2.2.1 Matrix Norm and Phase mean squared errors

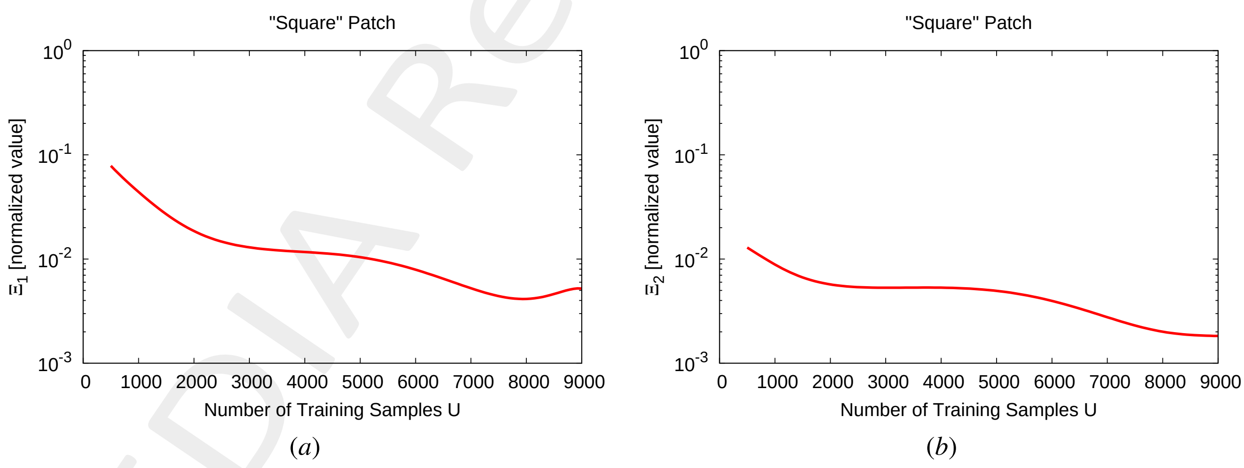

Figure 3: Square Patch Reflectarray 25×25 - Accuracy vs. Training Samples: Matrix norm error (a) and Phase mean squared error (b).

2.2.2 True vs. Predicted

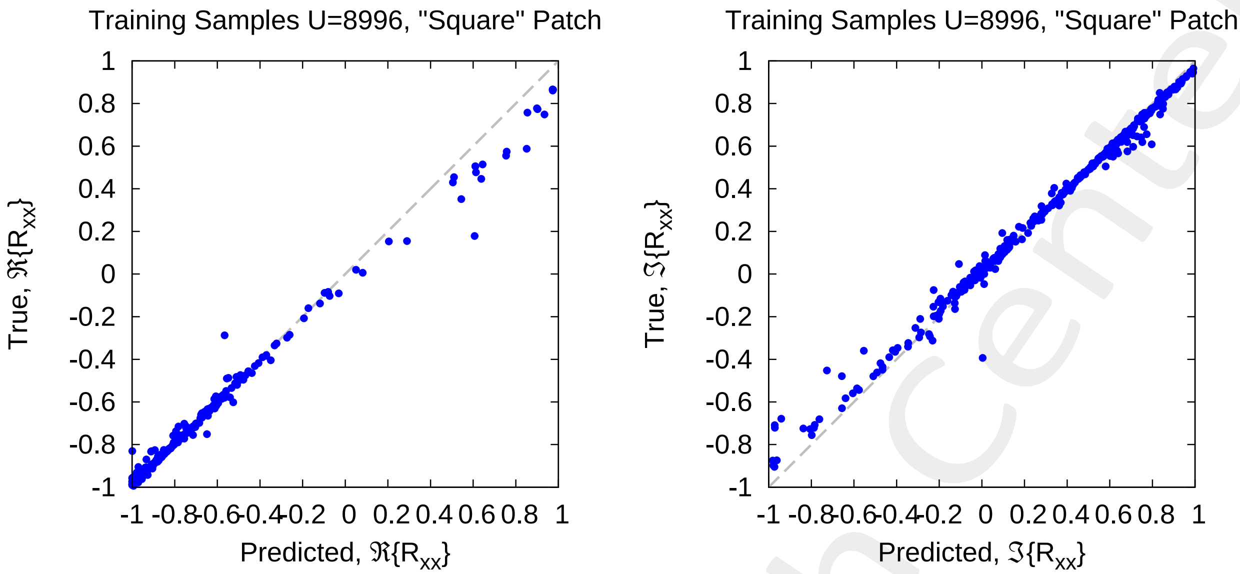

(a) (b)

Figure 4: Square Patch Reflectarray 25×25 - Accuracy vs. Training Samples - R_{xx}: Real (a) and Imaginary (b) part of true vs. predited.

2.3 Optimization target

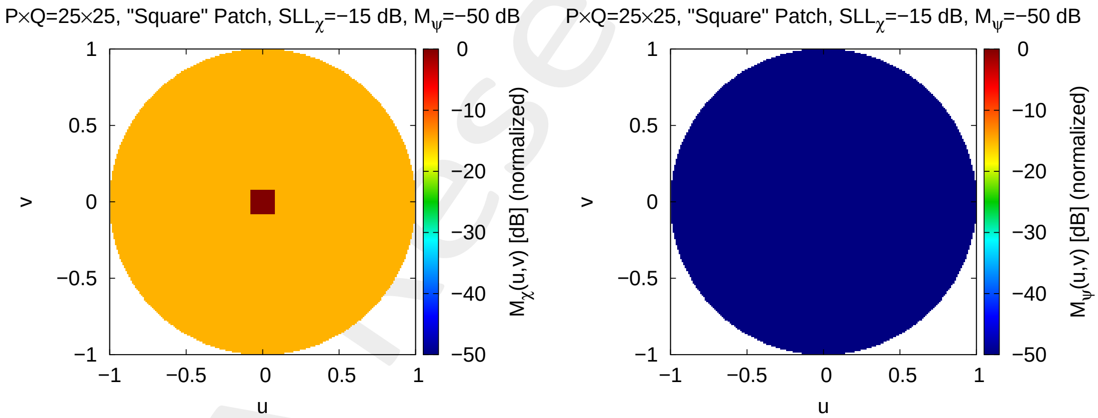

(a) (b)

Figure 5: Square Patch Reflectarray 25×25 - Optimization target: SLL on the wanted polarization(a), mask on the unwanted polarization (b).

2.4 Optimization results

2.4.1 Cost Function

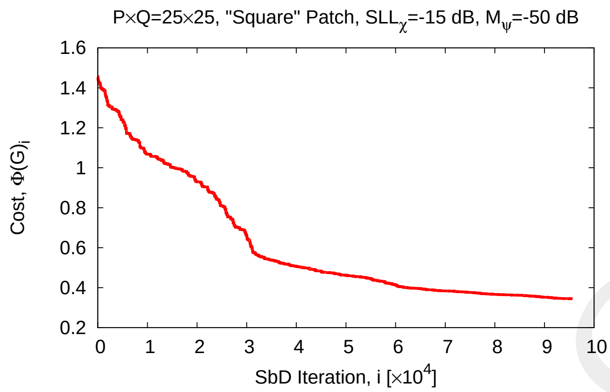

Figure 6: Square Patch Reflectarray 25×25 - Optimization: Cost function behavior.

2.4.2 Geometrical Design

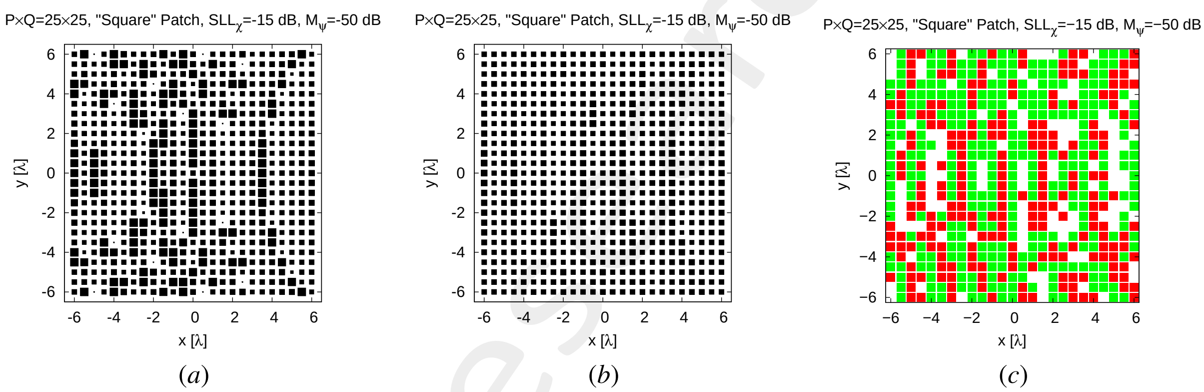

Figure 7: Square Patch Reflectarray 25×25 - Optimization: Starting reflectarray configuration(a), optimized reflectarray configuration (b) and the differential (c) betaween starting and optimal design.

2.4.3 Reflection Coefficient

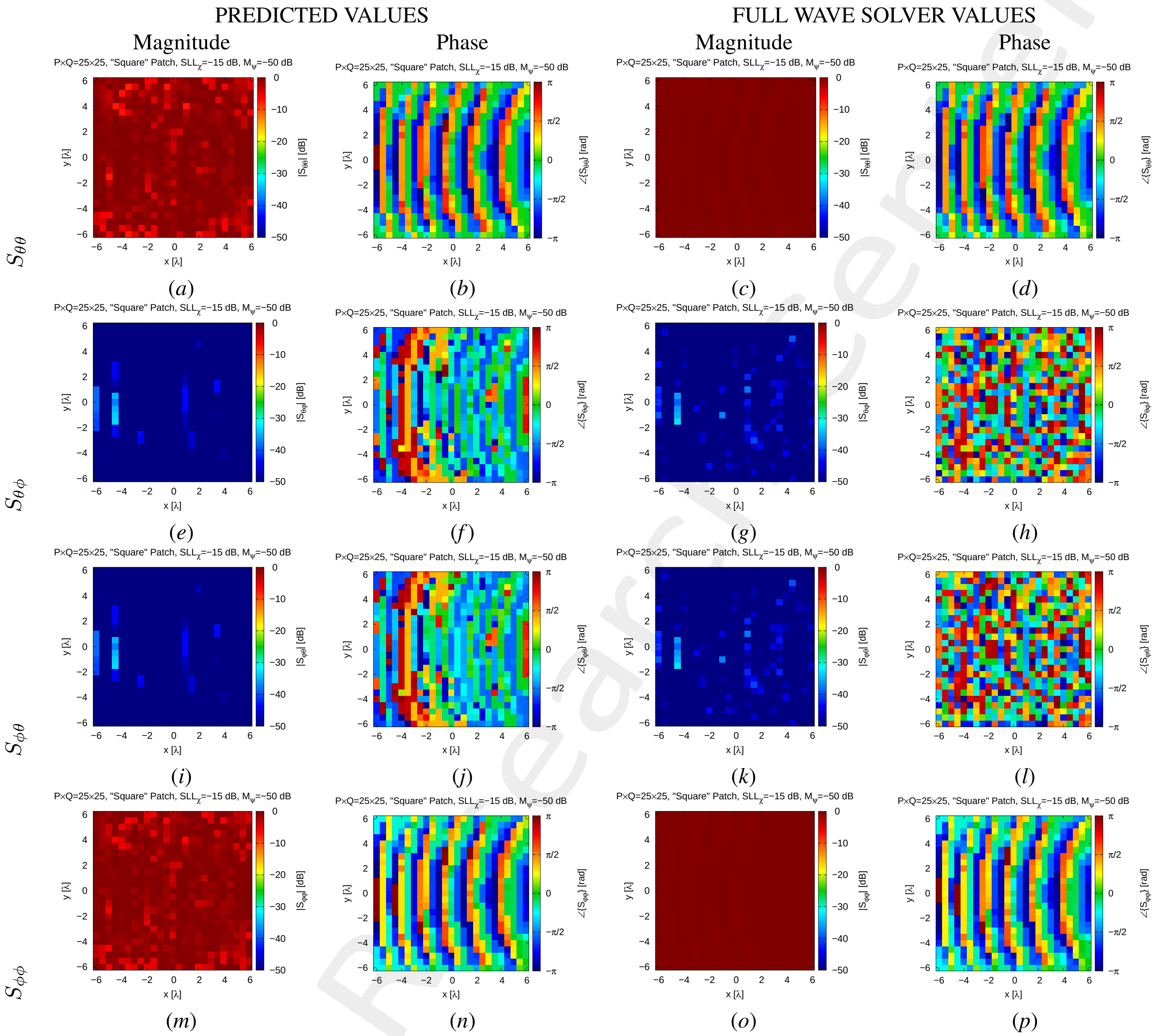

Figure 8: Square Patch Reflectarray 25×25 - Optimization - Reflection Coefficients: predicted(a)(b)(e)(f)(i)(j)(m)(n) vs. full-wave simulation (c)(d)(g)(h)(k)(l)(o)(p) of the magnitude(a)(c)(e)(g)(i)(k)(m)(o) and phase (b)(d)(f)(h)(j)(l)(n)(p) of $S_{\theta\theta}$(a)(b)(c)(d), $S_{\theta\phi}$(e)(f)(g)(h), $S_{\phi\theta}$(i)(j)(k)(l) and $S_{\phi\phi}$(m)(n)(o)(p).

2.4.4 Superficial Currents

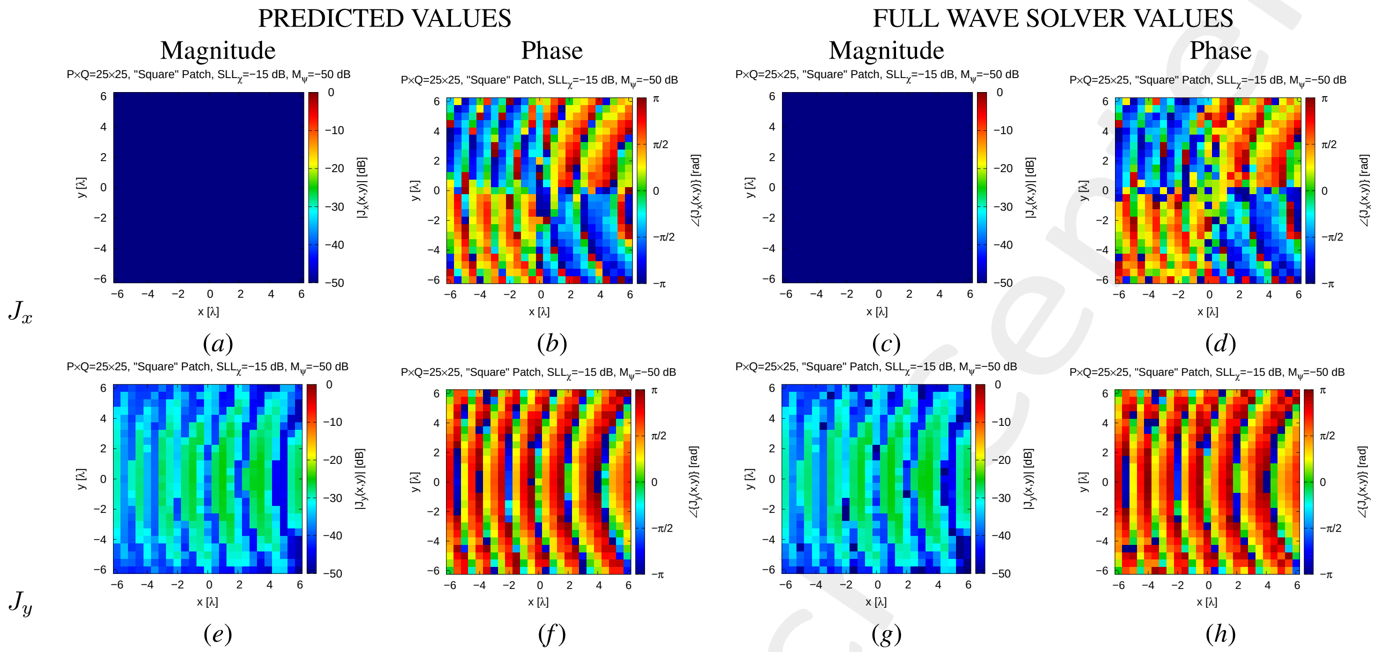

Figure 9: Square Patch Reflectarray 25 × 25 - Optimization - Superficial Currents: predicted(a)(b)(e)(f) vs. full-wave simulation (c)(d)(g)(h)of the magnitude(a)(c)(e)(g) and phase (b)(d)(f)(h) of J_x(a)(b)(c)(d) and J_y(e)(f)(g)(h).

2.4.5 Fields

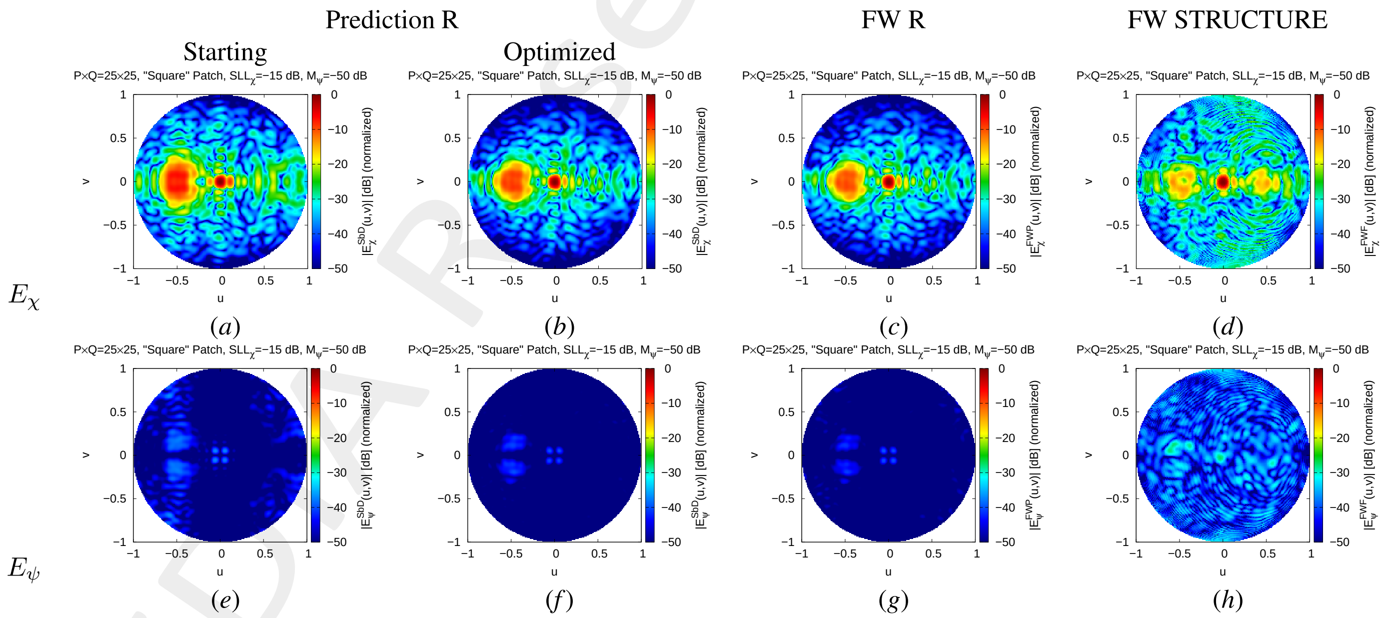

Figure 10: Square Patch Reflectarray 25 × 25 - Optimization - Radiated Fields: predicted(a)(b)(e)(f) vs. full-wave simulation of R (c)(g) vs. full-wave simulation of the entire structure (d)(h) of the magnitude of E_χ(a)(b)(c)(d) and E_ψ(e)(f)(g)(h).

2.4.6 Fields Cut

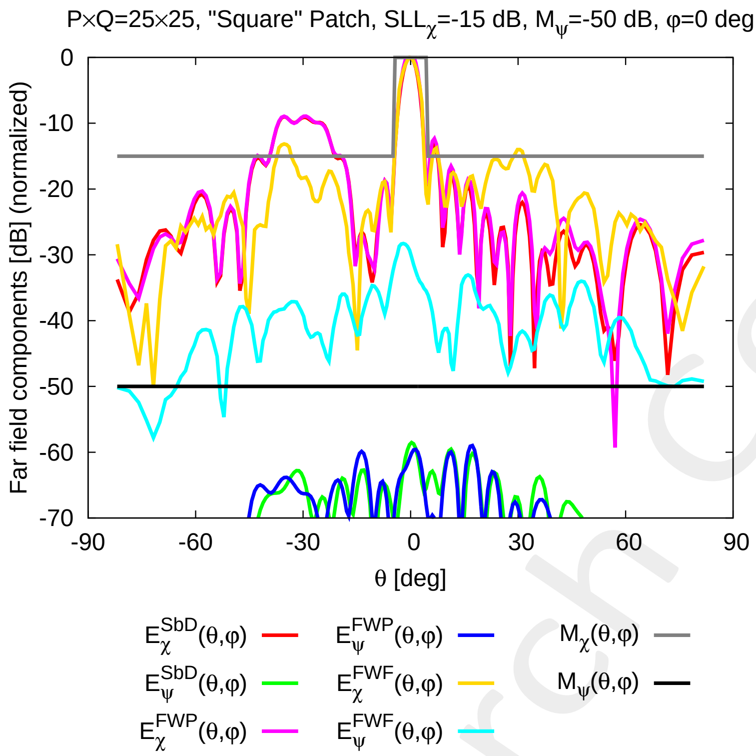

Figure 11: Square Patch Reflectarray 25×25 - Optimization - Radiated Field Cut with the comparison.

3 Square Patch Reflectarray: 25x25 - $R_f = 10$

3.1 Optimization target

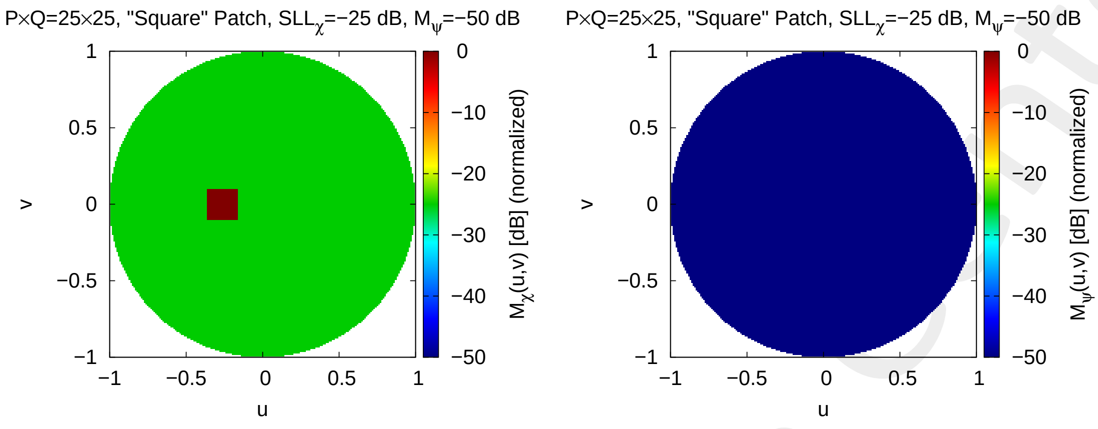

(a) (b)

Figure 12: Square Patch Reflectarray 25×25 $R_f = 10$ - Optimization target: SLL on the wanted polarization(a), mask on the unwanted polarization (b).

3.2 Optimization results

3.2.1 Cost Function

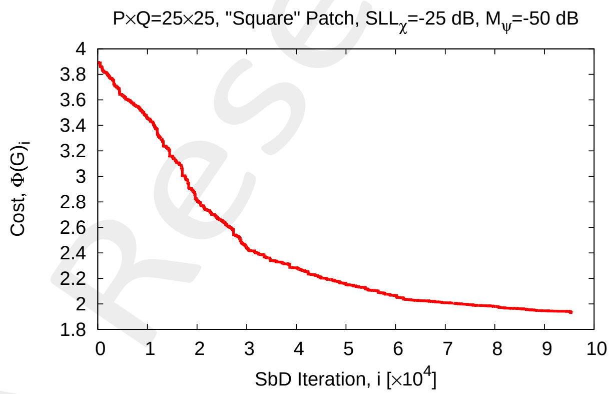

Figure 13: Square Patch Reflectarray $25 \times 25 R_f = 10$ - Optimization: Cost function behavior.

3.2.2 Geometrical Design

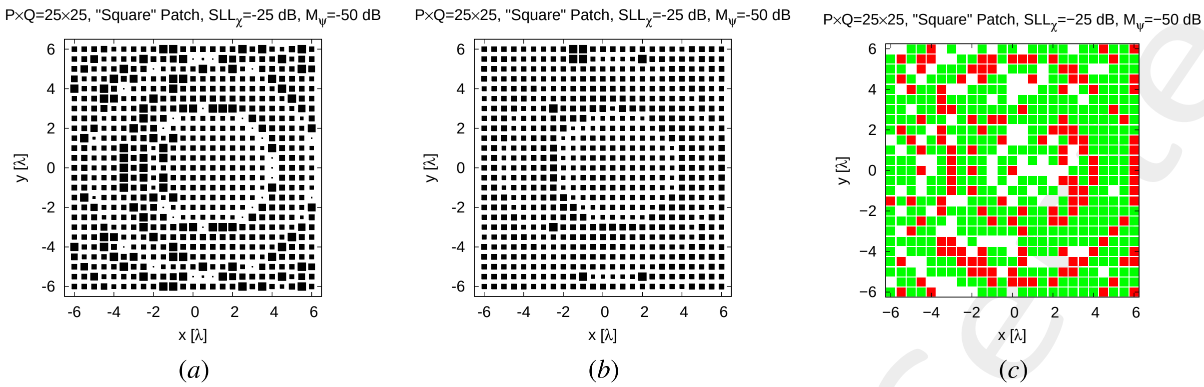

Figure 14: Square Patch Reflectarray $25 \times 25 R_f = 10$ - Optimization: Starting reflectarray configuration(a), optimized reflectarray configuration (b) and the differential (c) betaween starting and optimal design.

3.2.3 Reflection Coefficient

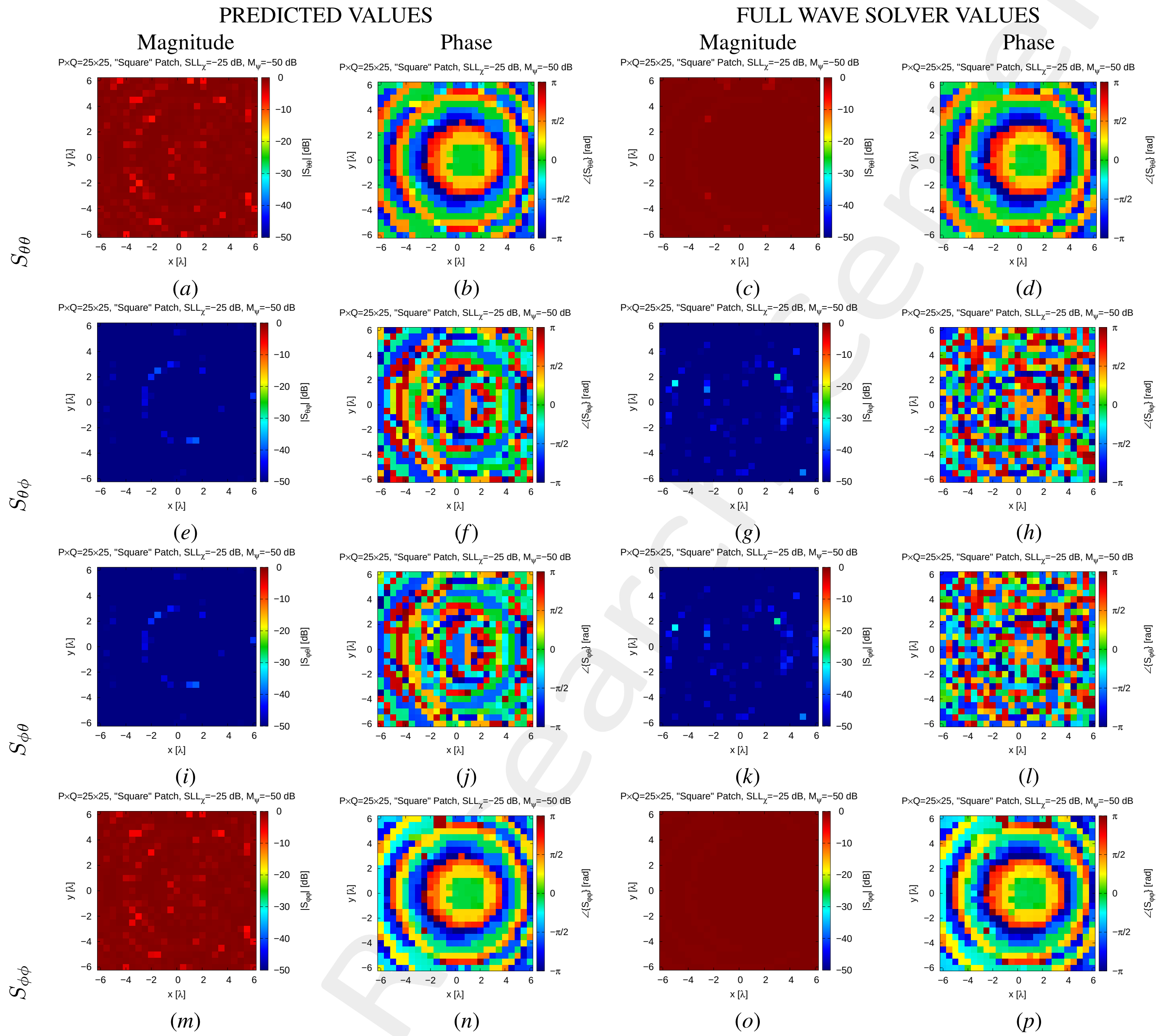

Figure 15: Square Patch Reflectarray 25×25 $R_f = 10$ - Optimization - Reflection Coefficients: predicted(a)(b)(e)(f)(i)(j)(m)(n) vs. full-wave simulation (c)(d)(g)(h)(k)(l)(o)(p) of the magnitude(a)(c)(e)(g)(i)(k)(m)(o) and phase (b)(d)(f)(h)(j)(l)(n)(p) of $S_{\theta\theta}$(a)(b)(c)(d), $S_{\theta\phi}$(e)(f)(g)(h), $S_{\phi\theta}$(i)(j)(k)(l) and $S_{\phi\phi}$(m)(n)(o)(p).

3.2.4 Superficial Currents

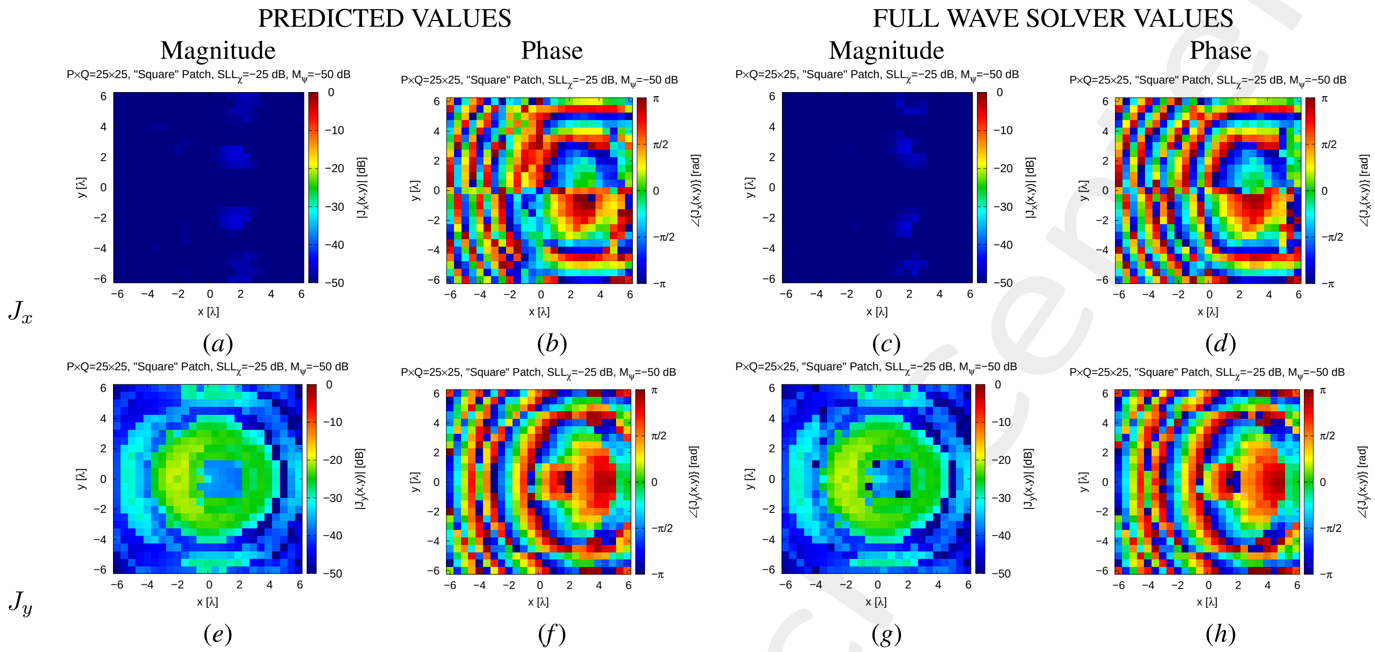

Figure 16: Square Patch Reflectarray 25×25 $R_f = 10$ - Optimization - Superficial Currents: predicted(a)(b)(e)(f) vs. full-wave simulation (c)(d)(g)(h)of the magnitude(a)(c)(e)(g) and phase (b)(d)(f)(h) of J_x(a)(b)(c)(d) and J_y(e)(f)(g)(h).

3.2.5 Fields

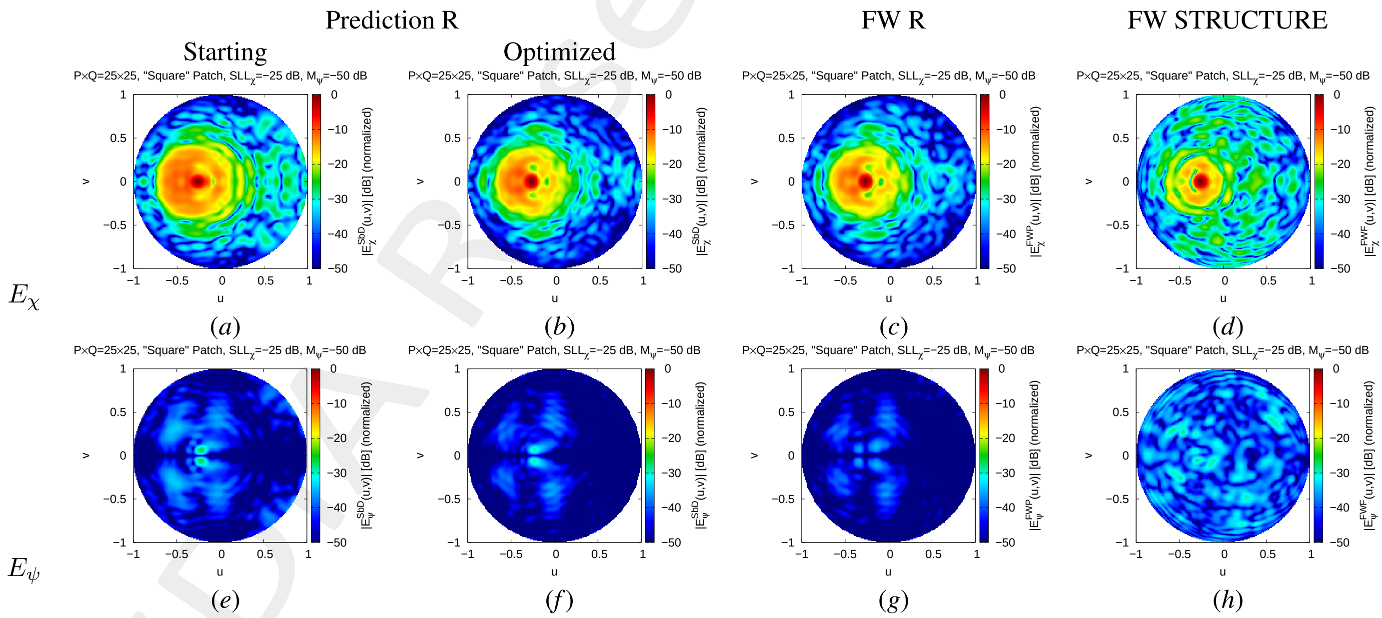

Figure 17: Square Patch Reflectarray 25×25 $R_f = 10$ - Optimization - Radiated Fields: predicted(a)(b)(e)(f) vs. full-wave simulation of R (c)(g) vs. full-wave simulation of the entire structure (d)(h) of the magnitude of E_χ(a)(b)(c)(d) and E_ψ(e)(f)(g)(h).

3.2.6 Fields Cut

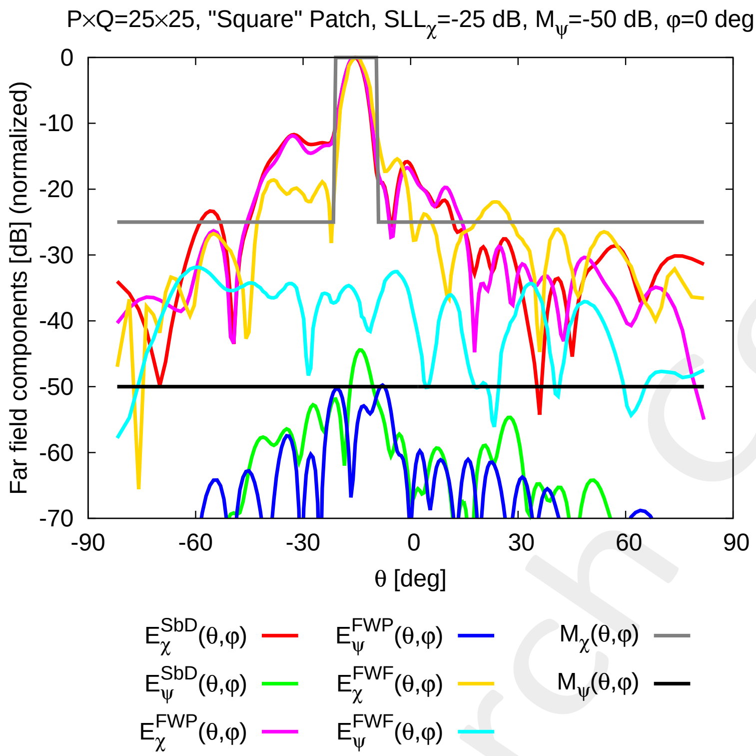

Figure 18: Square Patch Reflectarray 25×25 $R_f = 10$ - Optimization - Radiated Field Cut with the comparison.

More information on the topics of this document can be found in the following list of references.

References

[1] P. Rocca, M. Benedetti, M. Donelli, D. Franceschini, and A. Massa, “Evolutionary optimization as applied to inverse problems,” *Inverse Problems - 25 th Year Special Issue of Inverse Problems, Invited Topical Review*, vol. 25, pp. 1-41, Dec. 2009.

[2] P. Rocca, G. Oliveri, and A. Massa, “Differential Evolution as applied to electromagnetics,” *IEEE Antennas Propag. Mag.*, vol. 53, no. 1, pp. 38-49, Feb. 2011.

[3] P. Rocca, N. Anselmi, A. Polo, and A. Massa, “An irregular two-sizes square tiling method for the design of isophoric phased arrays,” *IEEE Trans. Antennas Propag.*, vol. 68, no. 6, pp. 4437-4449, Jun. 2020.

[4] P. Rocca, N. Anselmi, A. Polo, and A. Massa, “Modular design of hexagonal phased arrays through diamond tiles,” *IEEE Trans. Antennas Propag.*, vol.68, no. 5, pp. 3598-3612, May 2020.

[5] N. Anselmi, L. Poli, P. Rocca, and A. Massa, “Design of simplified array layouts for preliminary experimental testing and validation of large AESAs,” *IEEE Trans. Antennas Propag.*, vol. 66, no. 12, pp. 6906-6920, Dec. 2018.

[6] N. Anselmi, P. Rocca, M. Salucci, and A. Massa, “Contiguous phase-clustering in multibeam-on-receive scanning arrays.” *IEEE Trans. Antennas Propag.*, vol. 66, no. 11, pp. 5879-5891, Nov. 2018.

[7] G. Oliveri, G. Gottardi, F. Robol, A. Polo, L. Poli, M. Salucci, M. Chuan, C. Massagrande, P. Vinetti, M. Mattivi, R. Lombardi, and A. Massa, “Co-design of unconventional array architectures and antenna elements for 5G base station,” *IEEE Trans. Antennas Propag.*, vol. 65, no. 12, pp. 6752-6767, Dec. 2017.

[8] N. Anselmi, P. Rocca, M. Salucci, and A. Massa, “Irregular phased array tiling by means of analytic schemata-driven optimization,” *IEEE Trans. Antennas Propag.*, vol. 65, no. 9, pp. 4495-4510, September 2017.

[9] N. Anselmi, P. Rocca, M. Salucci, and A. Massa, “Optimization of excitation tolerances for robust beamforming in linear arrays,” *IET Microwaves, Antennas & Propagation*, vol. 10, no. 2, pp. 208-214, 2016.

[10] P. Rocca, R. J. Mailloux, and G. Toso, “GA-Based optimization of irregular sub-array layouts for wideband phased arrays desig,” *IEEE Antennas and Wireless Propag. Lett.*, vol. 14, pp. 131-134, 2015.

[11] P. Rocca, M. Donelli, G. Oliveri, F. Viani, and A. Massa, “Reconfigurable sum-difference pattern by means of parasitic elements for forward-looking monopulse radar,” *IET Radar, Sonar & Navigation*, vol 7, no. 7, pp. 747-754, 2013.

[12] P. Rocca, L. Manica, and A. Massa, “Ant colony based hybrid approach for optimal compromise sum-difference patterns synthesis,” *Microwave Opt. Technol. Lett.*, vol. 52, no. 1, pp. 128-132, Jan. 2010.

[13] P. Rocca, L. Manica, and A. Massa, “An improved excitation matching method based on an ant colony optimization for suboptimal-free clustering in sum-difference compromise synthesis,” *IEEE Trans. Antennas Propag.*, vol. 57, no. 8, pp. 2297-2306, Aug. 2009.

[14] P. Rocca, L. Manica, and A. Massa, "Hybrid approach for sub-arrayed monopulse antenna synthesis," *Electronics Letters*, vol. 44, no. 2, pp. 75-76, Jan. 2008.

[15] P. Rocca, L. Manica, F. Stringari, and A. Massa, "Ant colony optimization for tree-searching based synthesis of monopulse array antenna," *Electronics Letters*, vol. 44, no. 13, pp. 783-785, Jun. 19, 2008.

[16] G. Oliveri, A. Gelmini, A. Polo, N. Anselmi, and A. Massa, "System-by-design multi-scale synthesis of task-oriented reflectarrays," *IEEE Trans. Antennas Propag.*, vol. 68, no. 4, pp. 2867-2882, Apr. 2020.

[17] M. Salucci, F. Robol, N. Anselmi, M. A. Hannan, P. Rocca, G. Oliveri, M. Donelli, and A. Massa, "S-Band spline-shaped aperture-stacked patch antenna for air traffic control applications," *IEEE Tran. Antennas Propag.*, vol. 66, no. 8, pp. 4292-4297, Aug. 2018.

[18] M. Salucci, L. Poli, A. F. Morabito, and P. Rocca, "Adaptive nulling through subarray switching in planar antenna arrays," *Journal of Electromagnetic Waves and Applications*, vol. 30, no. 3, pp. 404-414, February 2016

[19] T. Moriyama, L. Poli, and P. Rocca, "Adaptive nulling in thinned planar arrays through genetic algorithms," *IEICE Electronics Express*, vol. 11, no. 21, pp. 1-9, Sep. 2014.

[20] L. Poli, P. Rocca, M. Salucci, and A. Massa, "Reconfigurable thinning for the adaptive control of linear arrays," *IEEE Trans. Antennas Propag.*, vol. 61, no. 10, pp. 5068-5077, Oct. 2013.

[21] P. Rocca, L. Poli, G. Oliveri, and A. Massa, "Adaptive nulling in time-varying scenarios through time-modulated linear arrays," *IEEE Antennas Wireless Propag. Lett.*, vol. 11, pp. 101-104, 2012.

[22] M. Benedetti, G. Oliveri, P. Rocca, and A. Massa, "A fully-adaptive smart antenna prototype: ideal model and experimental validation in complex interference scenarios," *Progress in Electromagnetic Research*, PIER 96, pp. 173-191, 2009.

[23] M. Benedetti, R. Azaro, and A. Massa, "Memory enhanced PSO-based optimization approach for smart antennas control in complex interference scenarios," *IEEE Trans. Antennas Propag.*, vol. 56, no. 7, pp. 1939-1947, Jul. 2008.

[24] M. Benedetti, R. Azaro, and A. Massa, "Experimental validation of a fully-adaptive smart antenna prototype," *Electronics Letters*, vol. 44, no. 11, pp. 661-662, May 2008.

[25] R. Azaro, L. Ioriatti, M. Martinelli, M. Benedetti, and A. Massa, "An experimental realization of a fully-adaptive smart antenna," *Microwave Opt. Technol. Lett.*, vol. 50, no. 6, pp. 1715-1716, Jun. 2008.

[26] M. Donelli, R. Azaro, L. Fimognari, and A. Massa, "A planar electronically reconfigurable Wi-Fi band antenna based on a parasitic microstrip structure," *IEEE Antennas Wireless Propag. Lett.*, vol. 6, pp. 623-626, 2007.

[27] M. Benedetti, R. Azaro, D. Franceschini, and A. Massa, "PSO-based real-time control of planar uniform circular arrays," *IEEE Antennas Wireless Propag. Lett.*, vol. 5, pp. 545-548, 2006.

[28] G. Oliveri, P. Rocca, M. Salucci, and A. Massa, "Holographic smart EM skins for advanced beam power shaping in next generation wireless environments," *IEEE J. Multiscale Multiphysics Comput. Tech.*, vol. 6, pp. 171-182, Oct. 2021.

[29] M. Salucci, L. Tenuti, G. Gottardi, A. Hannan, and A. Massa, "System-by-design method for efficient linear array miniaturisation through low-complexity isotropic lenses," *Electronic Letters*, vol. 55, no. 8, pp. 433-434, May 2019.

[30] M. Salucci, N. Anselmi, S. Goudos, and A. Massa, "Fast design of multiband fractal antennas through a system-by-design approach for NB-IoT applications," *EURASIP J. Wirel. Commun. Netw.*, vol. 2019, no. 1, pp. 68-83, Mar. 2019.

[31] M. Salucci, G. Oliveri, N. Anselmi, and A. Massa, "Material-by-design synthesis of conformal miniaturized linear phased arrays," *IEEE Access*, vol. 6, pp. 26367-26382, 2018.

[32] M. Salucci, G. Oliveri, N. Anselmi, G. Gottardi, and A. Massa, "Performance enhancement of linear active electronically-scanned arrays by means of MbD-synthesized metalenses," *Journal of Electromagnetic Waves and Applications*, vol. 32, no. 8, pp. 927-955, 2018.

[33] G. Oliveri, M. Salucci, N. Anselmi and A. Massa, "Multiscale System-by-Design synthesis of printed WAIMs for waveguide array enhancement," *IEEE J. Multiscale Multiphysics Computat. Techn.*, vol. 2, pp. 84-96, 2017.

[34] A. Massa and G. Oliveri, "Metamaterial-by-Design: Theory, methods, and applications to communications and sensing - Editorial," *EPJ Applied Metamaterials*, vol. 3, no. E1, pp. 1-3, 2016.

[35] G. Oliveri, F. Viani, N. Anselmi, and A. Massa, "Synthesis of multi-layer WAIM coatings for planar phased arrays within the system-by-design framework," *IEEE Trans. Antennas Propag.*, vol. 63, no. 6, pp. 2482-2496, June 2015.

[36] G. Oliveri, L. Tenuti, E. Bekele, M. Carlin, and A. Massa, "An SbD-QCTO approach to the synthesis of isotropic metamaterial lenses," *IEEE Antennas Wireless Propag. Lett.*, vol. 13, pp. 1783-1786, 2014.

[37] A. Massa, G. Oliveri, P. Rocca, and F. Viani, "System-by-Design: a new paradigm for handling design complexity," *8th European Conference on Antennas Propag. (EuCAP 2014)*, The Hague, The Netherlands, pp. 1180-1183, Apr. 6-11, 2014.

[38] P. Rocca, G. Oliveri, R. J. Mailloux, and A. Massa, "Unconventional phased array architectures and design Methodologies - A review," *Proceedings of the IEEE*, vol. 104, no. 3, pp. 544-560, March 2016.